Electronic Supporting Information (ESI)

Synthesis, DNA-binding and antiproliferative properties of diarylquinolizinium derivatives

Roberta Bortolozzi,[a] Heiko Ihmels,[*,b] Robin Schulte,[b] Christopher Stremmel,[b] Giampietro Viola[*,a]

Table of contents

1. Absorption and emission properties S2

2. DNA-binding properties S3

2.1. Spectrometric titrations S3

2.2. CD- and LD-spectroscopic analysis S6

2.3. ^{1}H- and ^{13}C-NMR spectra S9

1. Absorption and emission properties

Table S1. Absorption and emission properties of diarylquinolizinium derivates **3a**–**j**.

	3a				**3b**			
Solvent	λ_{abs}[a]	lg ε[b]	λ_{fl}[c]	Φ_{fl} / %[d]	λ_{abs}[a]	lg ε[b]	λ_{fl}[c]	Φ_{fl} / %[d]
MeOH	357	4.45	383	62	365	4.52	398	64
MeCN	358	4.45	382	58	364	4.45	399	60
$CHCl_3$	366	4.44	388	6	374	4.53	403	3
	3c				**3d**			
Solvent	λ_{abs}[a]	lg ε[b]	λ_{fl}[c]	Φ_{fl} / %[f]	λ_{abs}[a]	lg ε[b]	λ_{fl}[c]	Φ_{fl} / %[e]
MeOH	360	4.34	471	76	382	4.65	441	93
MeCN	359	4.29	474	70	381	4.56	447	87
$CHCl_3$	377	4.02	457	5	396	4.61	436	21
	3e				**3f**			
Solvent	λ_{abs}[a]	lg ε[b]	λ_{fl}[c]	Φ_{fl} / %[f]	λ_{abs}[a]	lg ε[b]	λ_{fl}[c]	Φ_{fl} / %[f]
MeOH	394	4.72	527	31	381	4.51	515	2
MeCN	391	4.68	511	40	380	4.59	520	4
$CHCl_3$	408	4.69	482	18	392	4.54	535	8
	3g				**3h**			
Solvent	λ_{abs}[a]	lg ε[b]	λ_{fl}[c]	Φ_{fl} / %[d]	λ_{abs}[a]	lg ε[b]	λ_{fl}[c]	Φ_{fl} / %[d]
MeOH	359	4.41	384	61	361	4.45	398	<1.0
MeCN	358	4.50	381	61	360	4.51	398	<1.0
$CHCl_3$	–	–	–	–	–	–	–	–

	3i				**3j**			
Solvent	λ_{abs}[a]	lg ε[b]	λ_{fl}[c]	Φ_{fl} / %[d]	λ_{abs}[a]	lg ε[b]	λ_{fl}[c]	Φ_{fl} / %[e]
MeOH	359	4.41	384	61	387	4.69	437	92
MeCN	358	4.50	381	61	390	4.65	450	76
$CHCl_3$	–	–	–	–	390	4.71	432	19

[a] Long-wavelength absorption maxima in nm, c = 20 µM. [b] Molar extinction coefficient in cm^{-1} M^{-1}. [c] Fluorescence emission maximum with Abs. = 0.1 at excitation wavelength; **3a**, **3b**, **3g**, and **3h**: λ_{ex} = 330 nm; **3c**–**f**, and **3j**: λ_{ex} = 380 nm. [d] Fluorescence quantum yield relative to coumarin 120 (ref. 1). [e] Fluorescence quantum yield relative to coumarin 1 (Ref. 2). [f]Fluorescence quantum yield relative to coumarin 102 (Ref. 2).

[1] H. Pal, S. Nad, and M. Kumbhakar, *J. Chem. Phys.* 2003, **119**, 443.
[2] G. Jones, W. R. Jackson, C. Y. Choi, and W. R. Bergmark, *J. Phys. Chem.* 1985, **89**, 294.

2. DNA-binding properties

2.1. Spectrometric titrations

All DNA titrations were performed in BPE buffer (pH = 7.0; with 5% DMSO). The titrant solution contained the same ligand concentration as the analyte solution, to ensure a constant ligand concentration throughout the titration. The excitation wavelength in the fluorimetric titrations was λ_{ex} = 330 nm for the ligands **3a**, **3b**, **3g**, and **3h** and λ_{ex} = 380 nm the ligands **3c**–**f**, and **3j**. After recording the pure ligand solution, small aliquots of DNA solution were titrated to the ligand solution until no significant change in absorbance or fluorescence intensity was observed. The spectra were recorded after an equilibration time of 3 min.

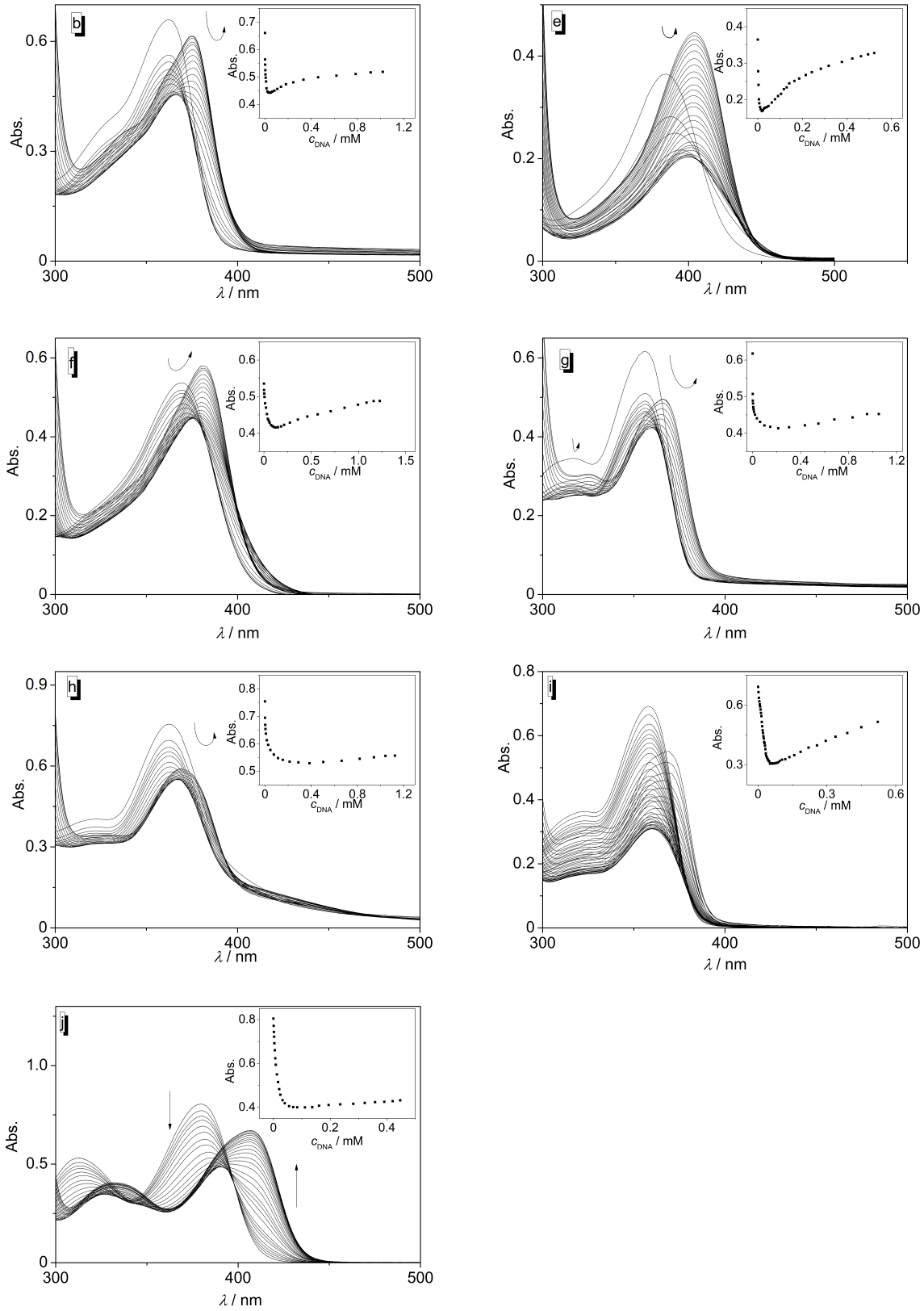

Figure S1. Photometric titration of **3b** (b), **3e** (e), **3f** (f), **3g** (g), **3h** (h), **3i** (i), and **3j** (j) (c = 20 µM) with ct DNA (c = 2.0 mM in base pairs) in BPE buffer (pH = 7.0; 5% v/v DMSO). The arrows indicate the development of the absorption bands during titration. Inset: Plot of absorption Abs. versus c_{DNA}.

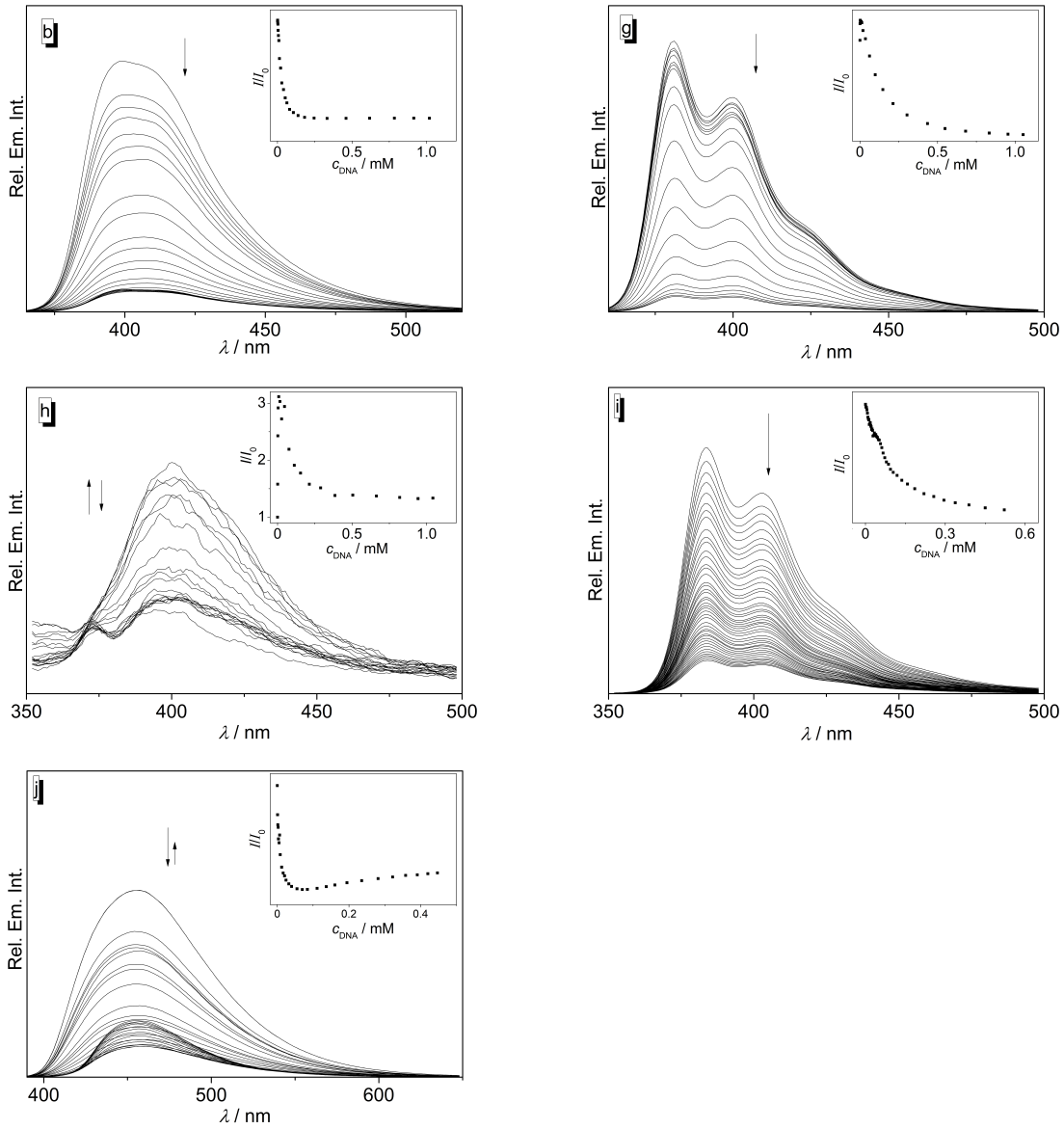

Figure S2. Fluorimetric titration of **3b** (b), **3g** (g), **3h** (h), **3i** (i) and **3j** (j) (c = 20 µM) with ct DNA (c = 2.0 mM in base pairs) in BPE buffer (pH = 7.0; 5% v/v DMSO). The arrows indicate the development of the emission bands during titration. Inset: Plot of normalized emission intensity I / I_0 versus c_{DNA}.

The data from the fluorimetric (**3a**, **3c**, **3e**, **3f**, **3g**, and **3i**) or photometric (**3b**, **3d**, and **3j**) were used to calculate the binding constants by fitting the data to the theoretical model.[3,4] Therefor the datapoints were displayed as Scatchard plots and numerically fitted to the neighbor exclusion model of McGhee and von Hippel (eq. 1, Figure S3). The fitting was calculated with the implemented Levenberg-Marquardt non-linear curve fitting algorithm of Origin 8.5.1.

[3] J. D. McGhee, P. H. von Hippel, *J. Mol. Biol.* 1974, **86**, 469–489.
[4] A. Granzhan, H. Ihmels and G. Viola, *J. Am. Chem. Soc.* 2007, **129**, 1254–1267.

$$\frac{r}{c} = K(1 - nr)\left(\frac{1 - nr}{1 - (n-1)r}\right)^{n-1} \qquad \text{(eq. 1)}$$

r = ratio of bound ligand molecules per DNA base pair: $r = \frac{c_b}{c_{DNA}}$ (eq. 2)

c = concentration of the unbound ligand: $c = c_L - c_b$ (eq. 3)

c_b: concentration of the DNA-bound ligand: $c_b = c_L \times \frac{A_f - A}{A_f - A_b}$ (eq. 4)

A_f is the absorbance/emission of the free ligand at a given wavelength, A_b is the absorbance/emission of the bound ligand, and A is the absorbance/emission at a given ligand-to-DNA ratio.

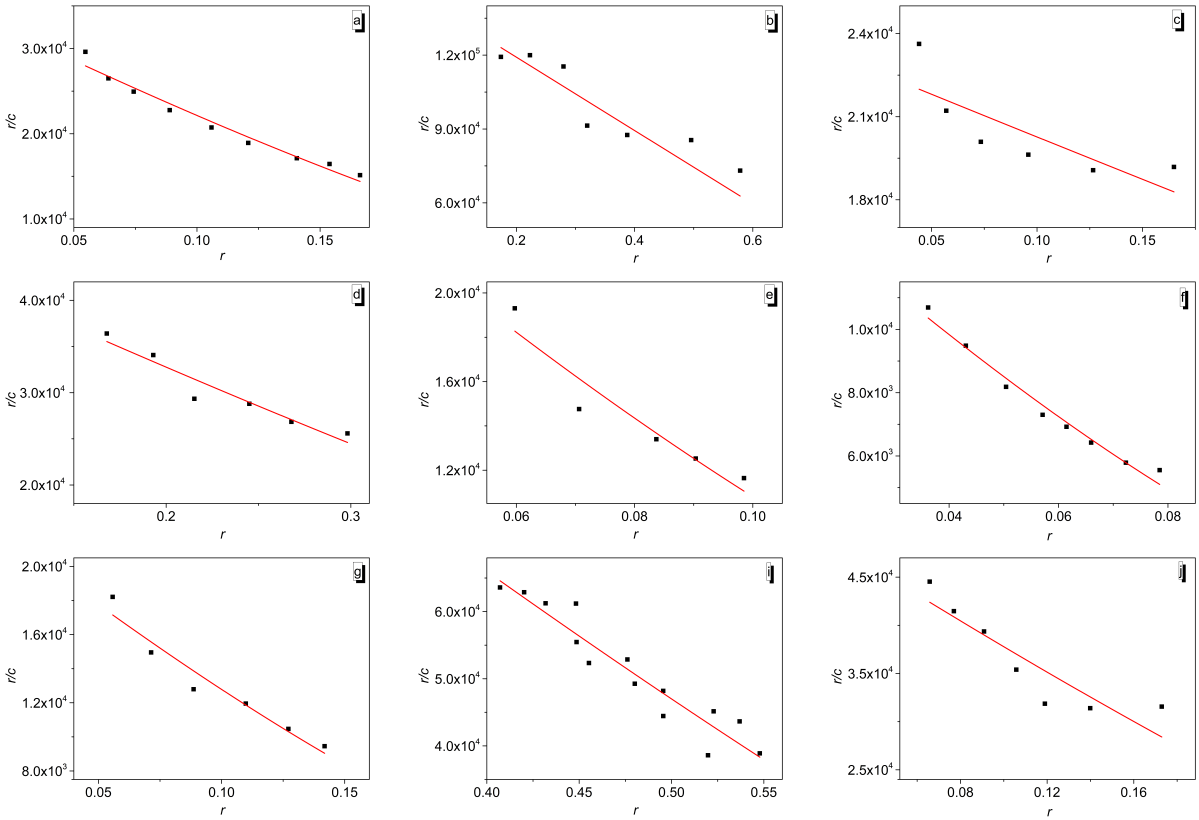

Figure S3. Scatchard plot of *r*/*c versus r* from spectrofluorimetric titration of ct DNA to **3a** (a), **3c** (c), **3e** (e), **3f** (f), **3g** (g), and **3i** (i) and from spectrophotometric titration of ct DNA to **3b** (b) and **3d** (d), and **3j** (j) and fit of the experimental data to the theoretical model.

2.2. CD- and LD-spectroscopic analysis

The following setup was used to record the CD and LD spectra:

Wavelength range	230–500 nm
Bandwidth	1.0 nm
Scan rate	1.0 nm/s
Time per datapoint	0.5 s
Temperature	20 °C

The solutions were prepared according to Table S2 and S3 and measured after an equilibration time of 30 min.

Table S2. Composition of samples for CD-spectroscopic measurements.

Sample[a]	c_{Ligand}/µM	V_{Ligand}/µL[b]	*LDR*
1	0	0	0
2	1.0	2.0	0.05
3	4.0	8.0	0.20
4	10	20	0.50
5	20	40	1.00

[a] c_{DNA} = 20 µM; V_{DNA} = 200 µL; *V*(buffer) = 1700 µL *V*(DMSO) = 100 µL; [b] c_0(Ligang) = 1.00 mM in MeOH, Solvent was removed prior to the addition of DMSO, DNA and buffer.

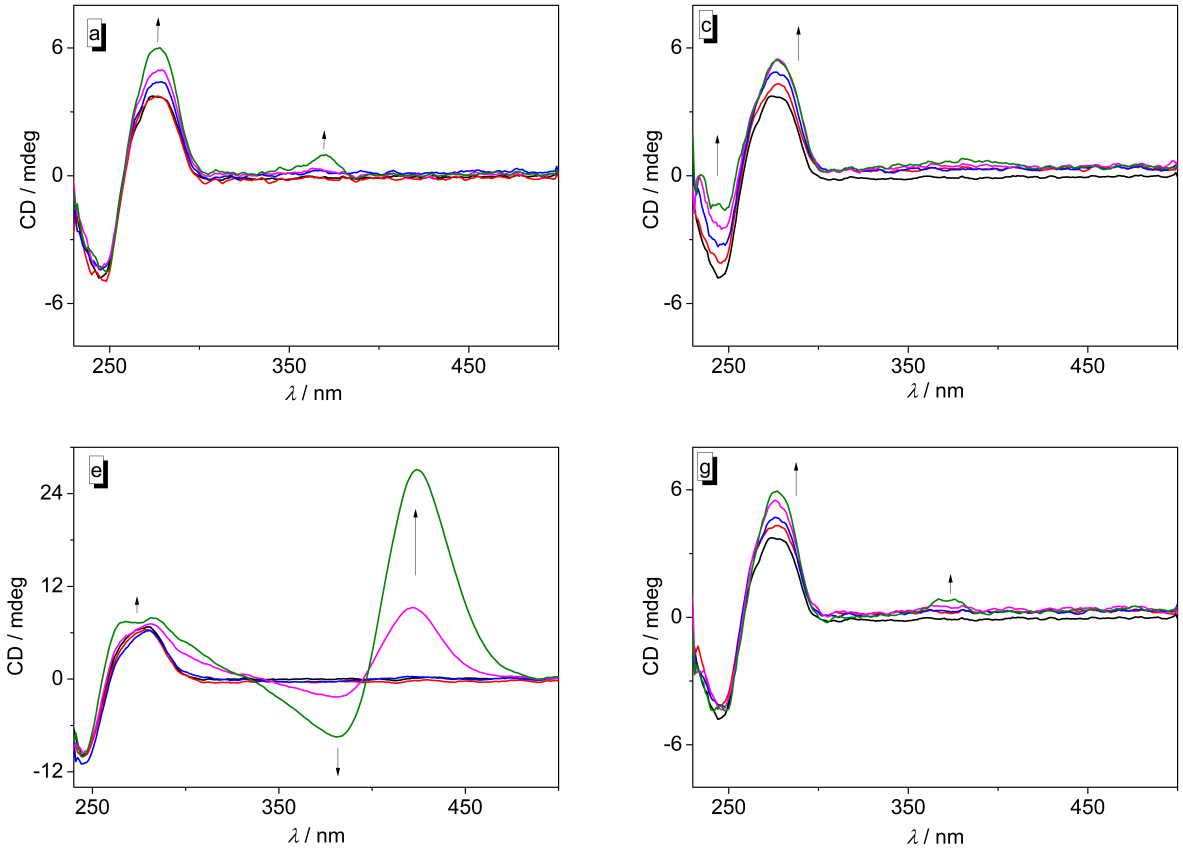

Figure S4. CD spectra of the ligands **3a** (a), **3c** (c), **3e** (e), and **3g** (g), in the presence of ct DNA in BPE buffer (pH = 7.00, 5% DMSO) at *LDR* 0.00 (black), 0.05 (red), 0.20 (blue), 0.50 (magenta), and 1.00 (green); c_{DNA} = 20 µM; *T* = 20 °C. The arrows indicate the development of the CD bands with increasing *LDR*.

Table S3. Composition of samples for *flow*-LD-spectroscopic measurements.

Sample[a]	c_{Ligand}/µM	V_{Ligand}/µL[b]	*LDR*
1	0	0	0
2	1.0	1.0	0.05
3	4.0	4.0	0.20
4	10	10	0.50
5	20	20	1.00

[a] c_{DNA} = 20 µM; V_{DNA} = 100 µL; *V*(buffer) = 850 µL *V*(DMSO) = 50 µL; [b] c_0(Ligang) = 1.00 mM in MeOH, Solvent was removed prior to the addition of DMSO, DNA and buffer.

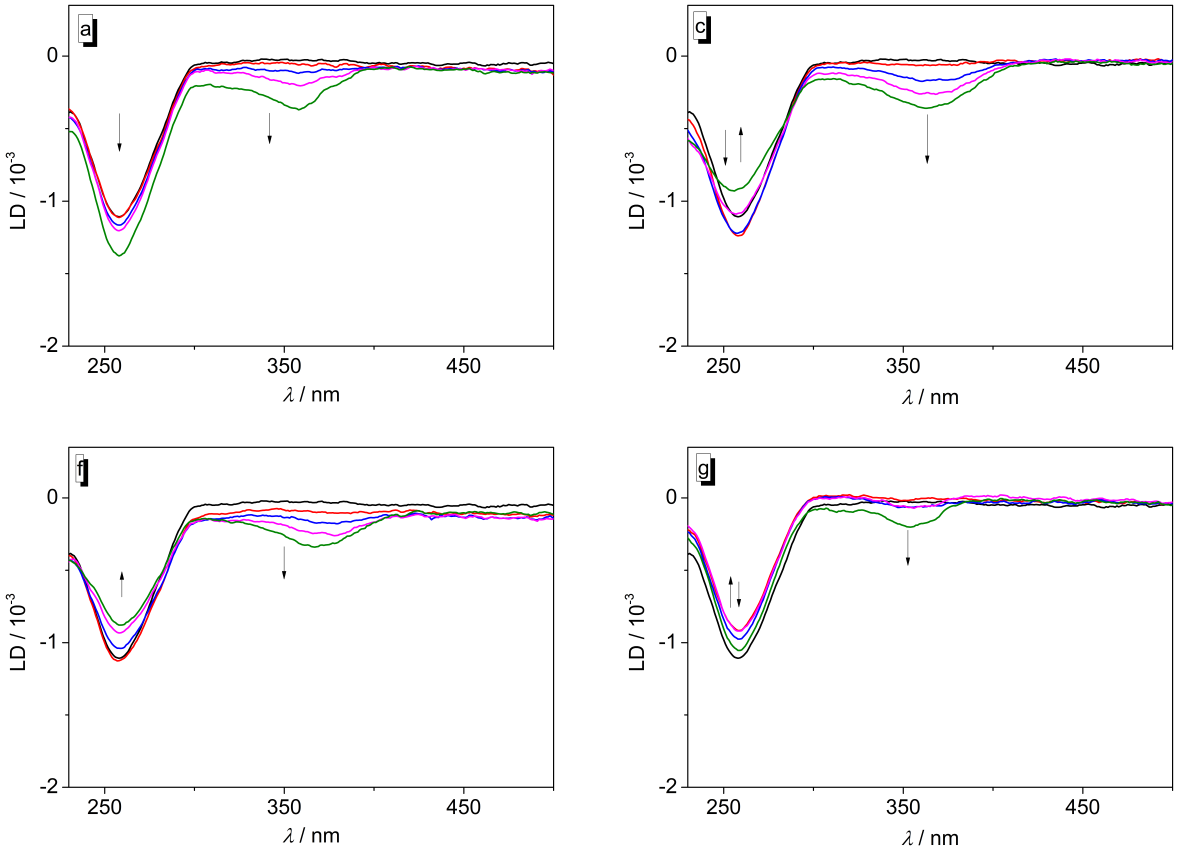

Figure S5. LD spectra of the ligands **3a** (a), **3c** (c), **3f** (f), and **3g** (g), in the presence of ct DNA in BPE buffer (pH = 7.00, 5% DMSO) at *LDR* 0.00 (black), 0.05 (red), 0.20 (blue), 0.50 (magenta), and 1.00 (green); c_{DNA} = 20 µM; *T* = 20 °C. The arrows indicate the development of the CD bands with increasing *LDR*.

2.3. ^{1}H- and ^{13}C-NMR spectra

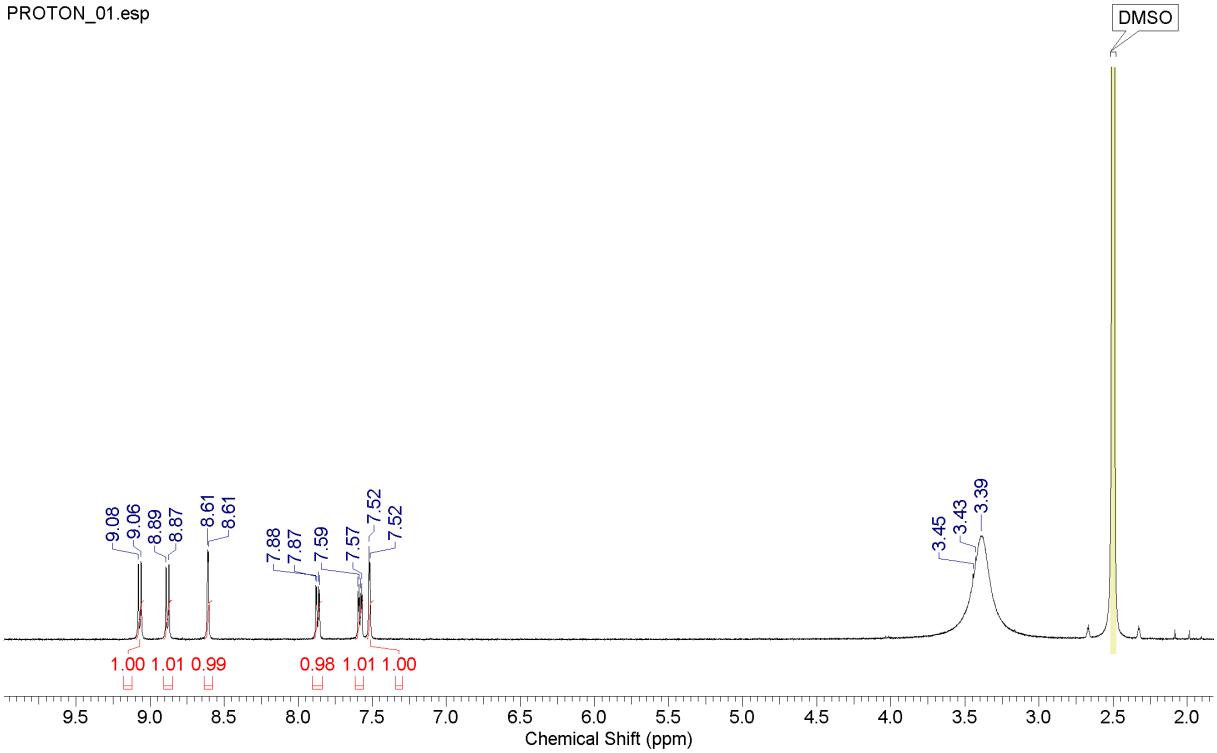

Figure S6. ^{1}H-NMR spectrum of compound **7** in DMSO-d_6 (600 MHz).

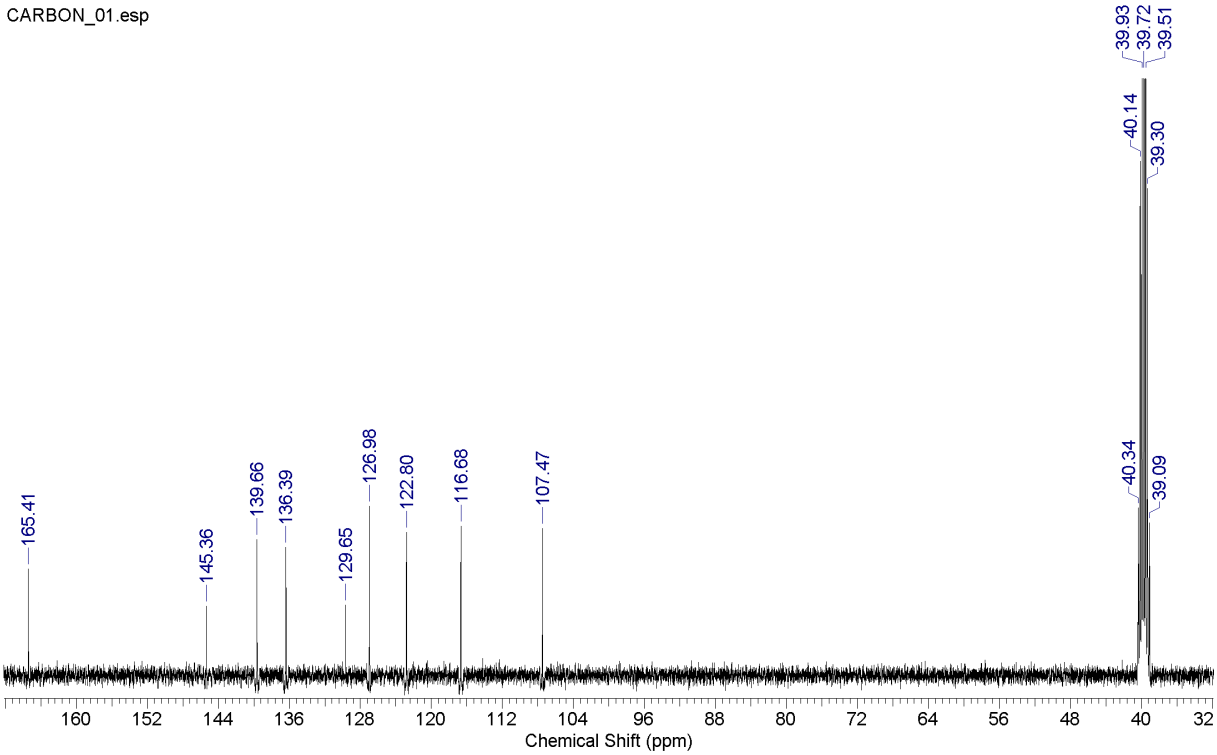

Figure S7. ^{13}C-NMR spectrum of compound **7** in DMSO-d_6 (150 MHz).

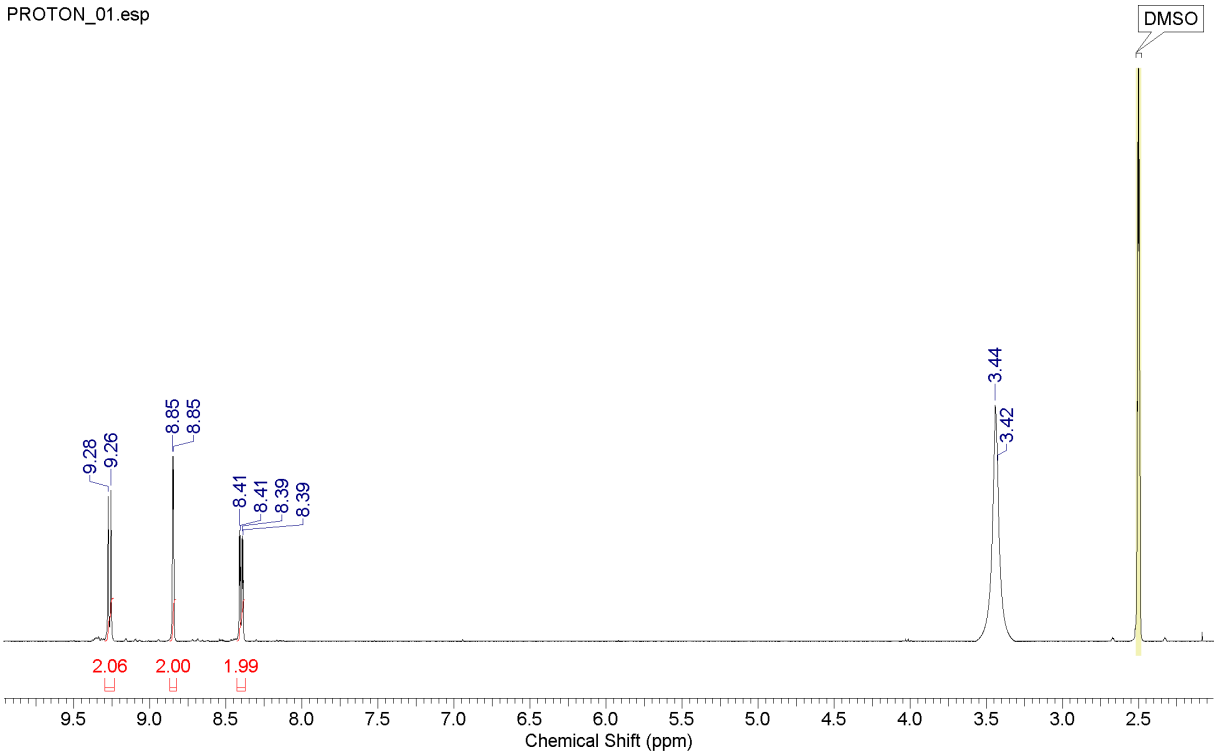

Figure S8. ^{1}H-NMR spectrum of compound **1b** in DMSO-d_6 (600 MHz).

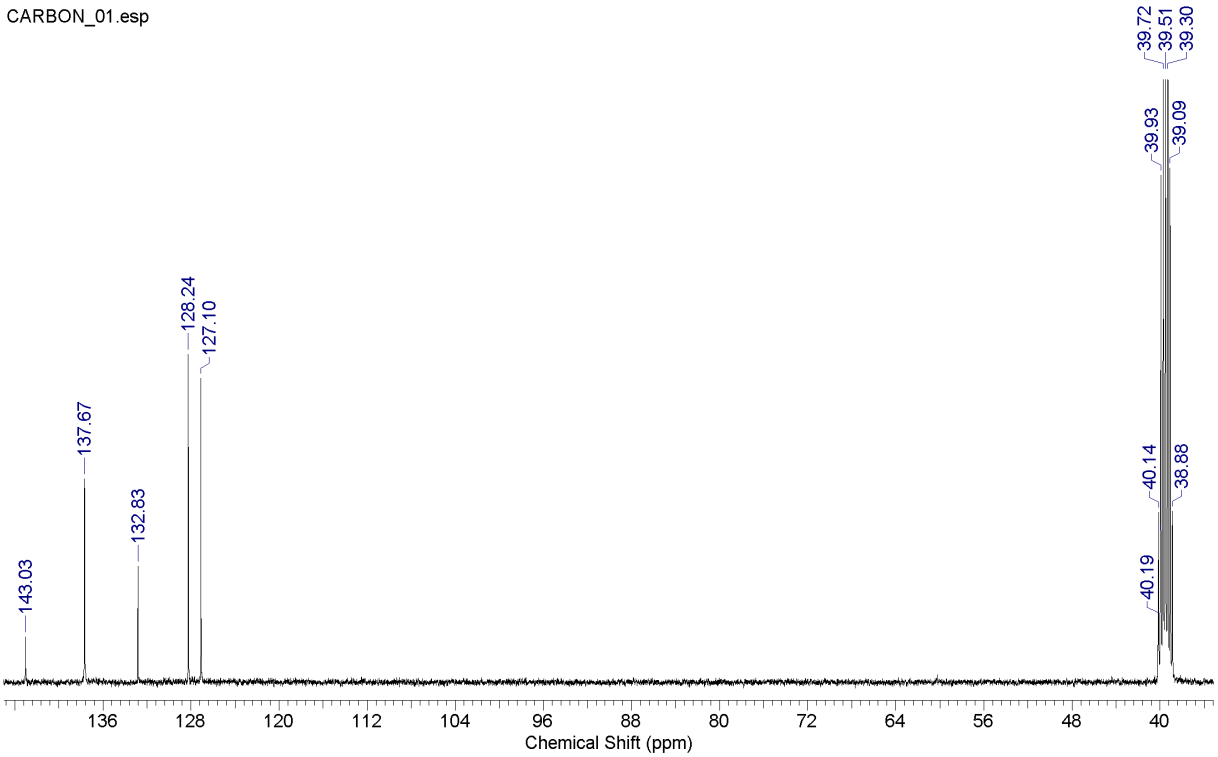

Figure S9. ^{13}C-NMR spectrum of compound **1b** in DMSO-d_6 (150 MHz).

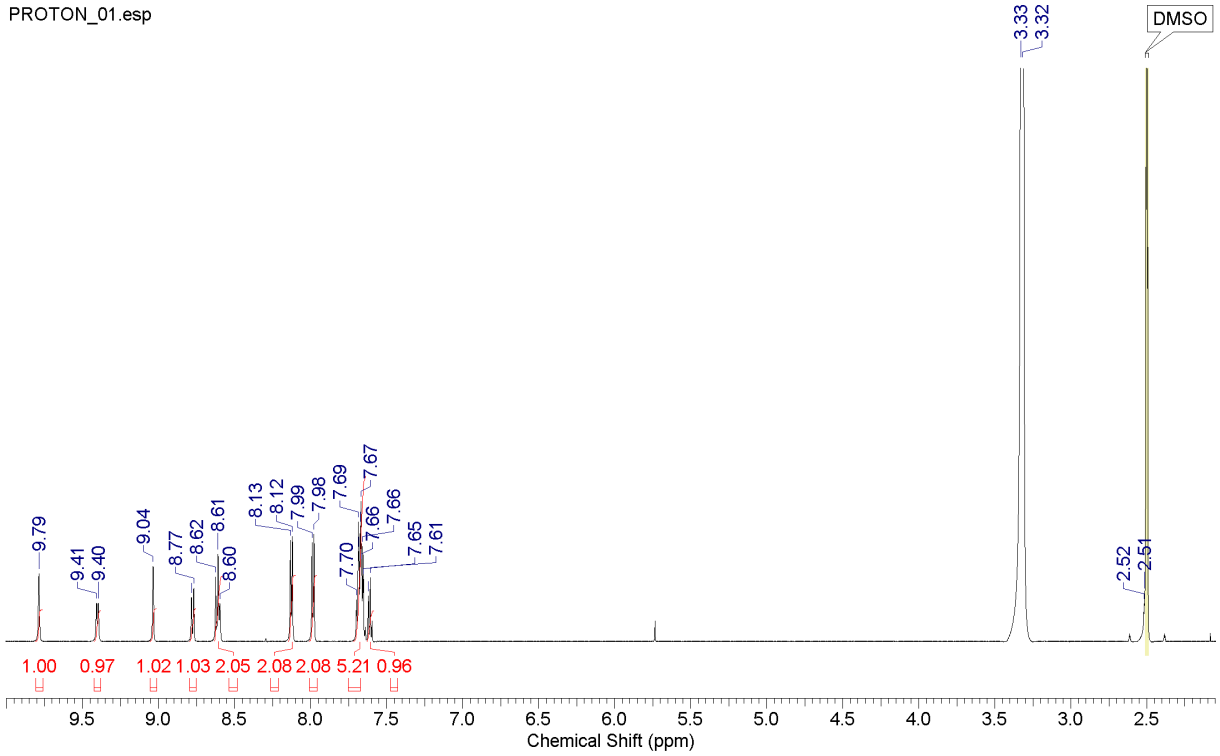

Figure S10. ^{1}H-NMR spectrum of compound **3a** in DMSO-d_6 (600 MHz).

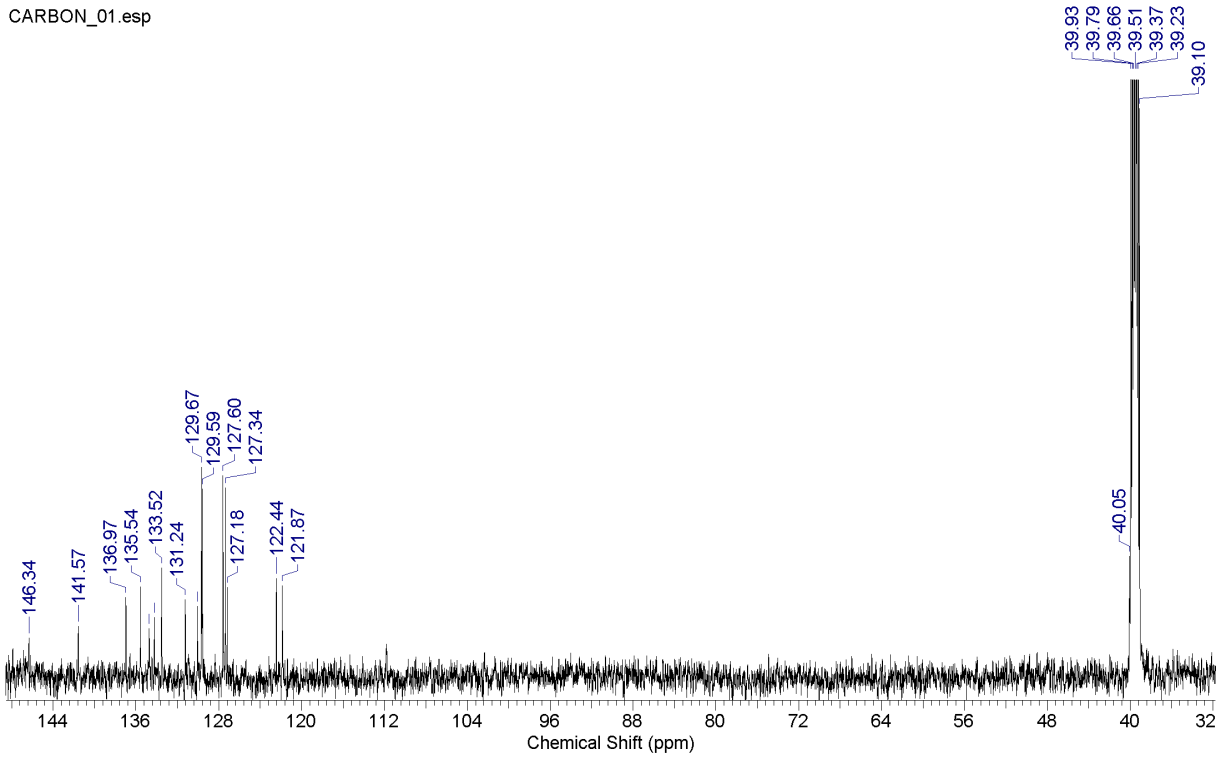

Figure S11. ^{13}C-NMR spectrum of compound **3a** in DMSO-d_6 (150 MHz).

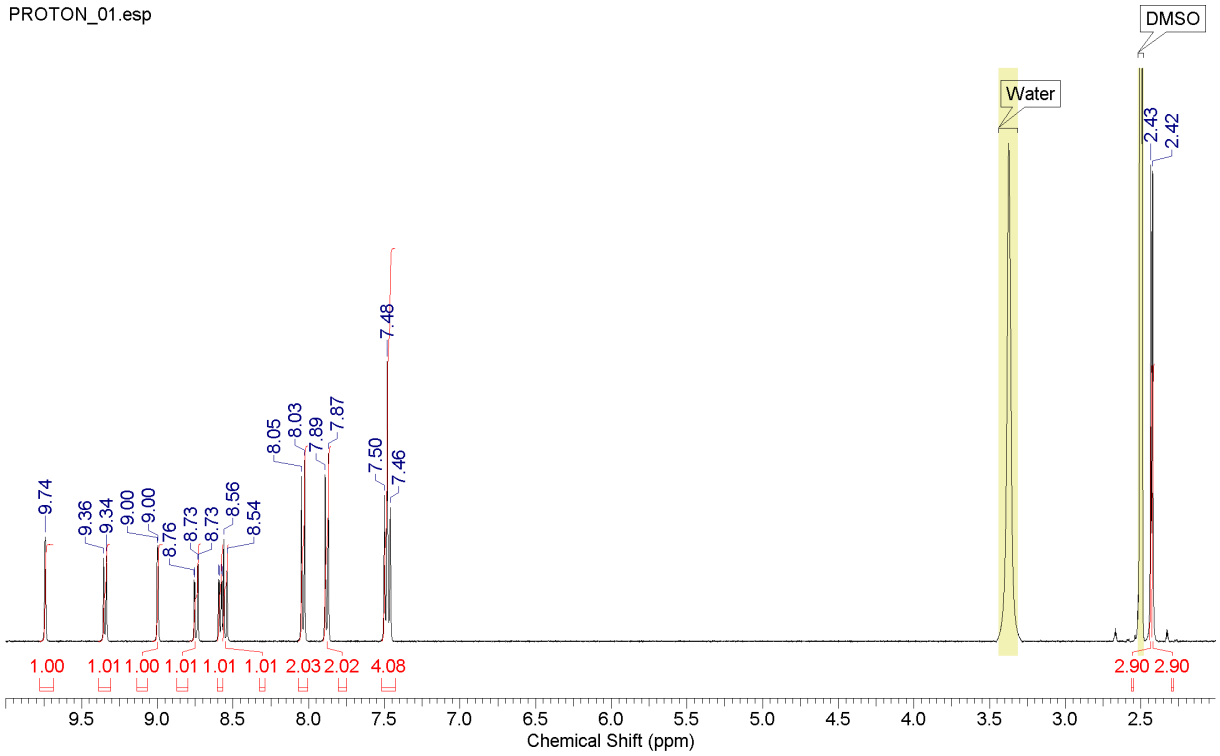

Figure S12. ^{1}H-NMR spectrum of compound **3b** in DMSO-d_6 (600 MHz).

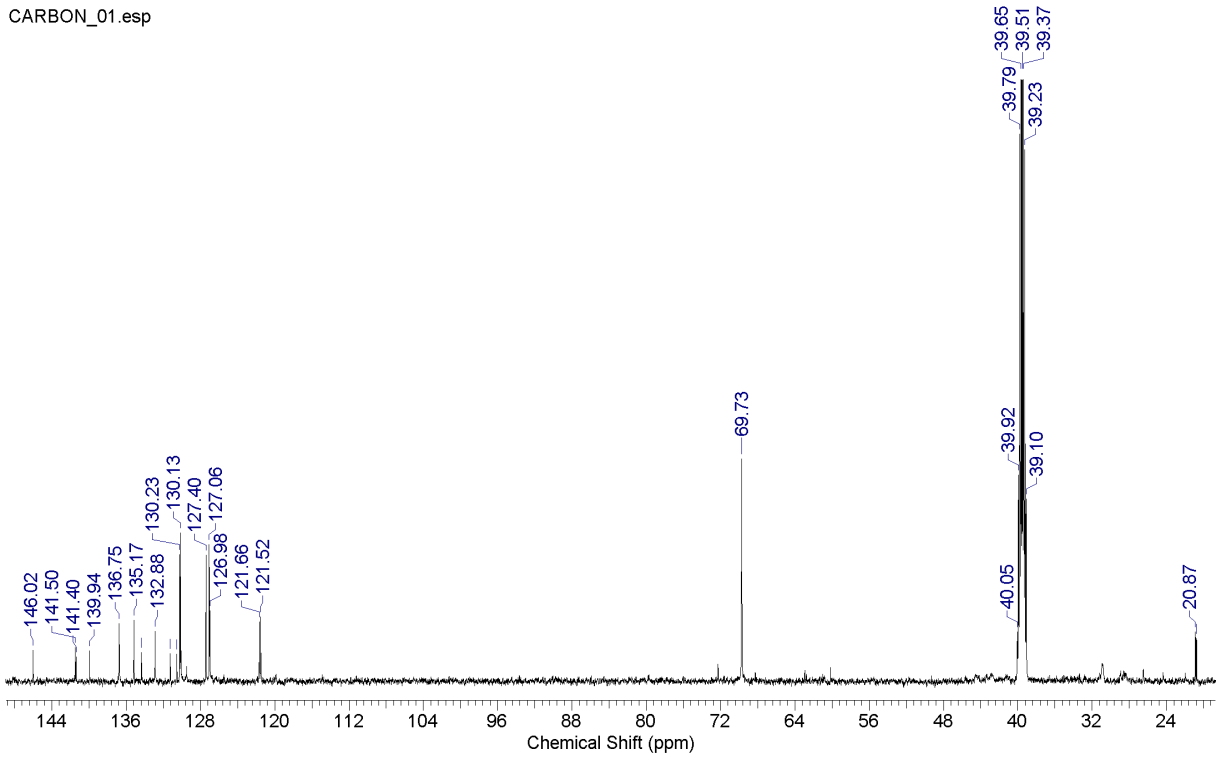

Figure S13. ^{13}C-NMR spectrum of compound **3b** in DMSO-d_6 (150 MHz).

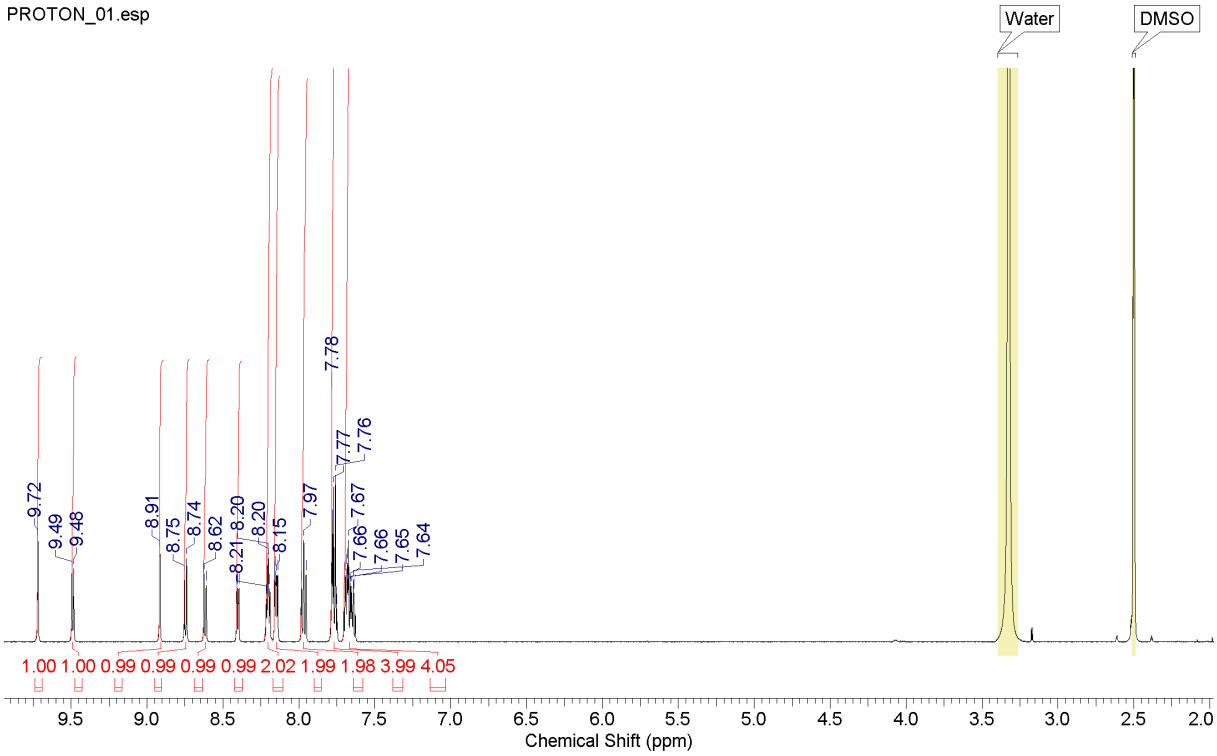

Figure S14. ^{1}H-NMR spectrum of compound **3c** in DMSO-d_6 (600 MHz).

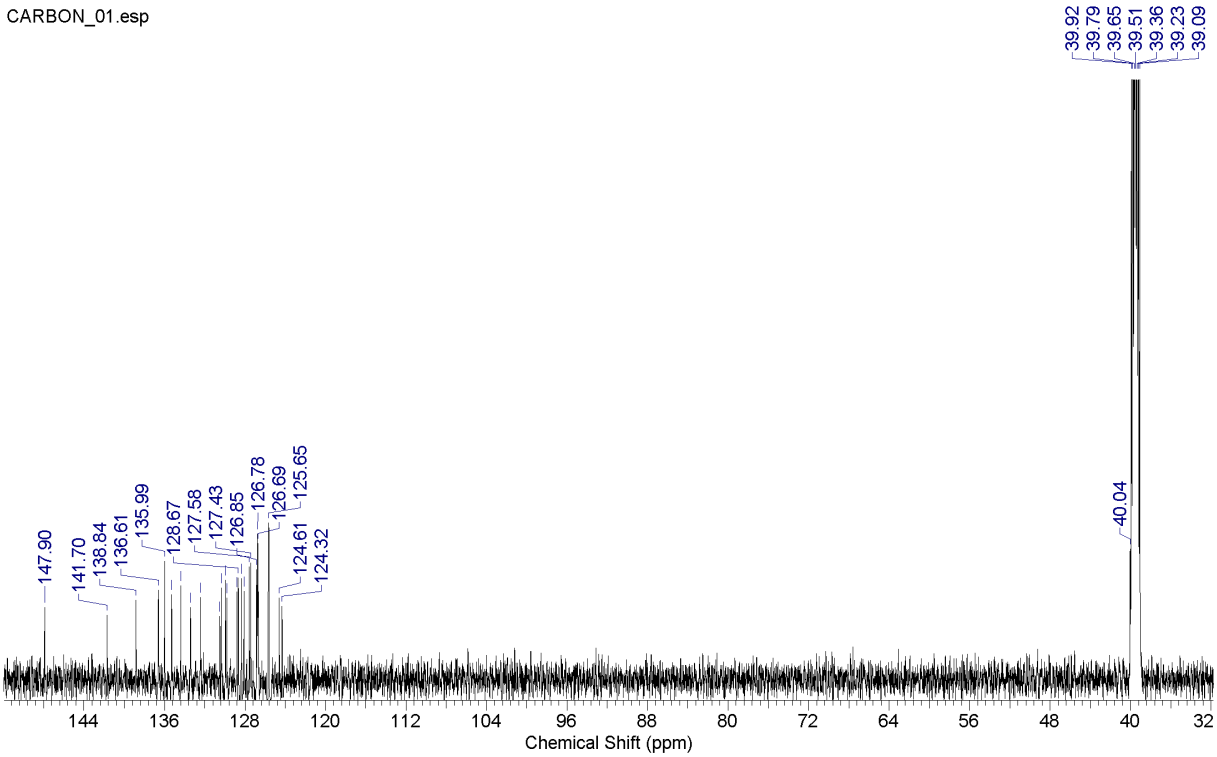

Figure S15 ^{13}C-NMR spectrum of compound **3c** in DMSO-d_6 (150 MHz).

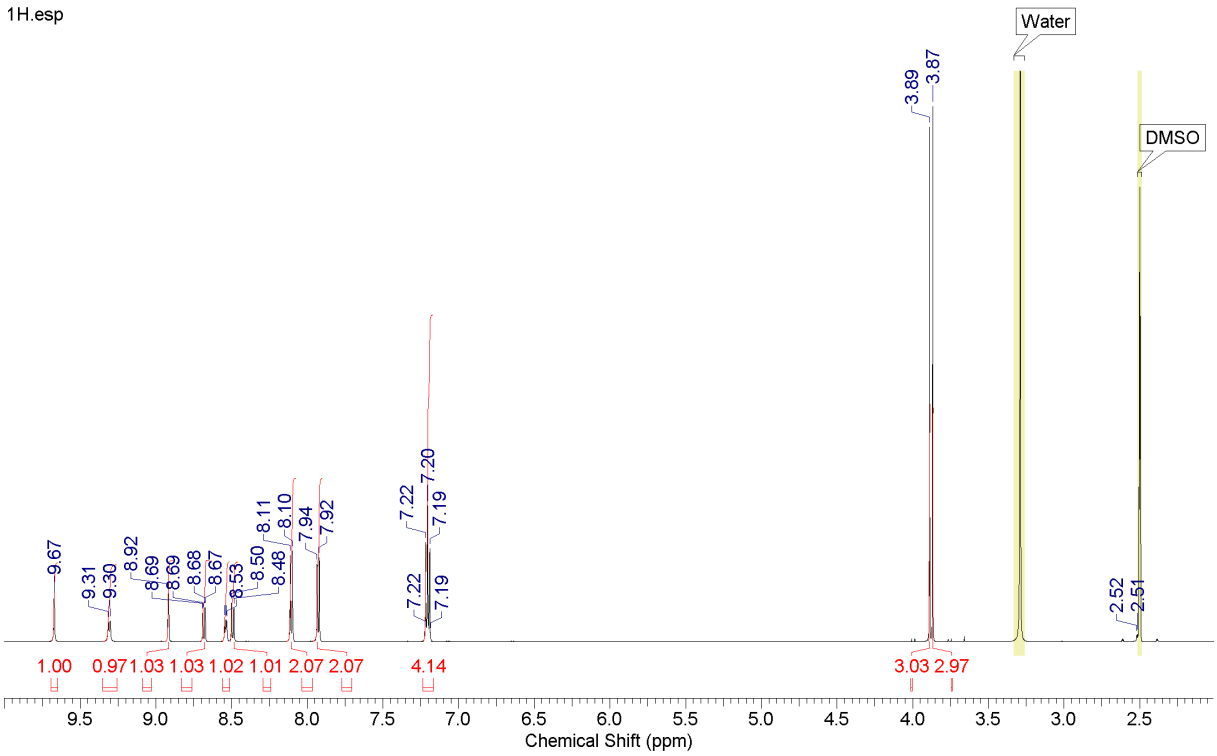

Figure S16. ^{1}H-NMR spectrum of compound **3d** in DMSO-d_6 (600 MHz).

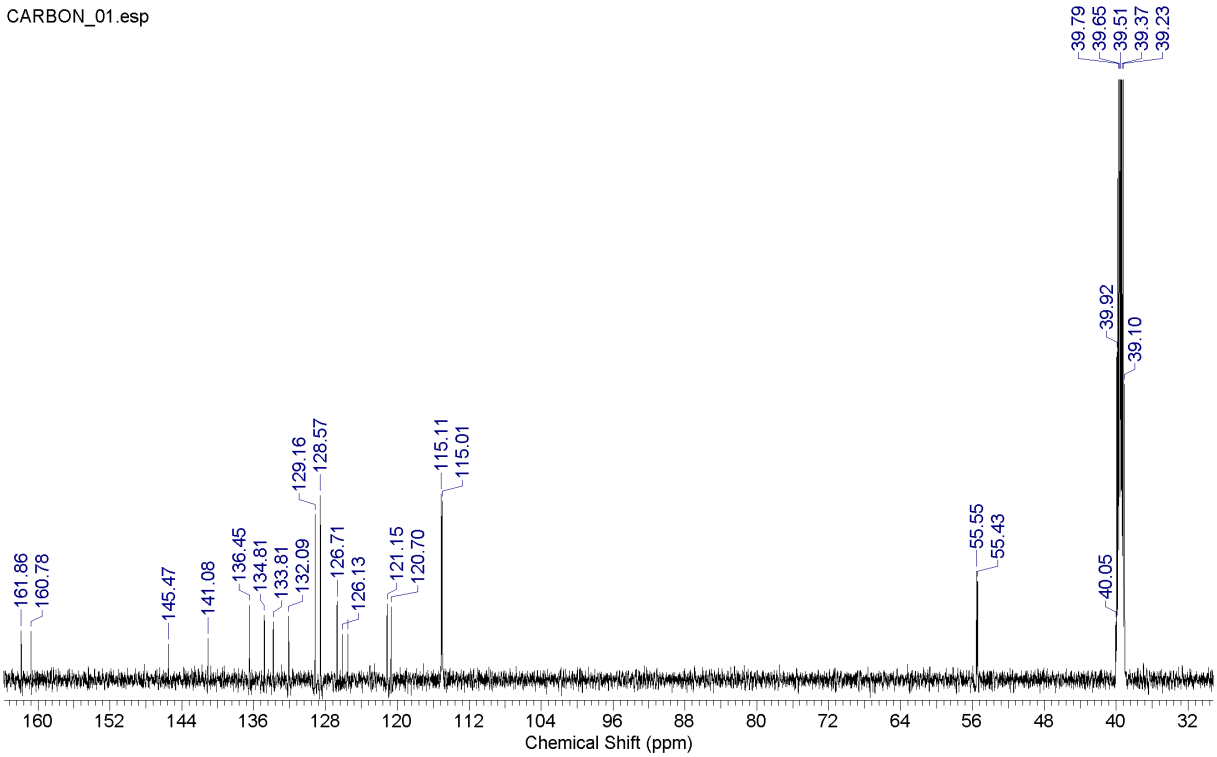

Figure S17. ^{13}C-NMR spectrum of compound **3d** in DMSO-d_6 (150 MHz).

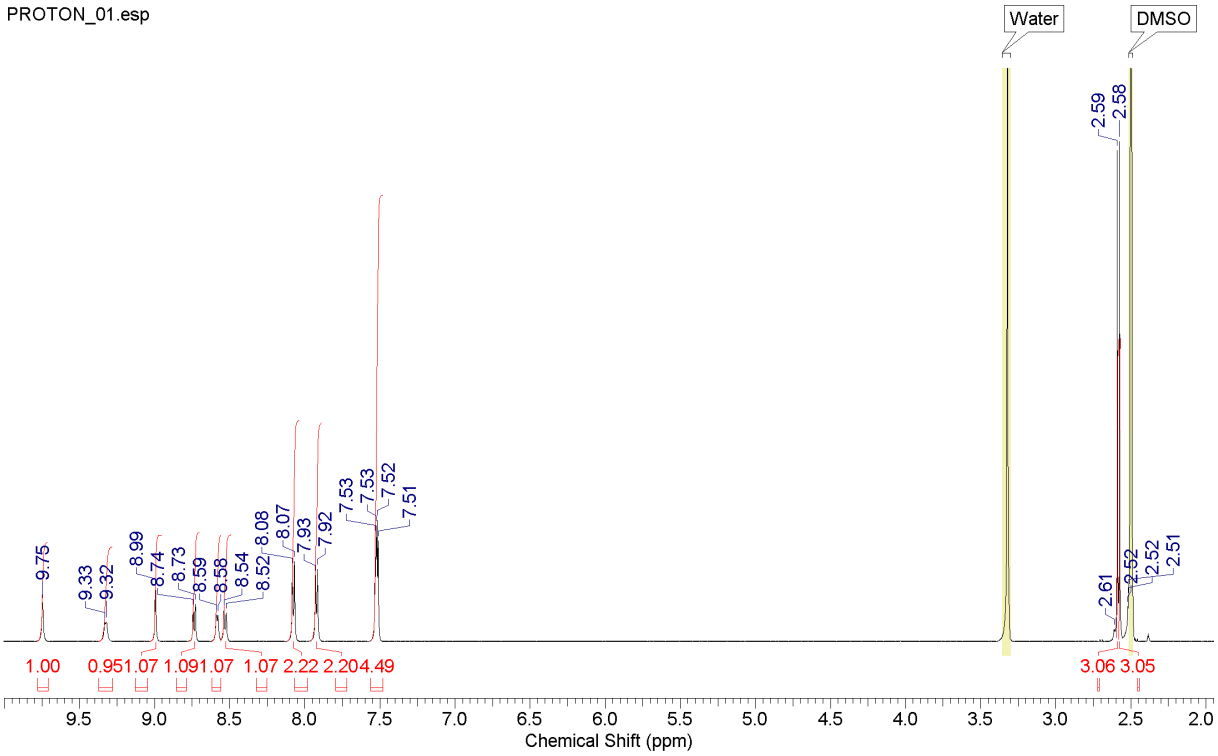

Figure S18. ^{1}H-NMR spectrum of compound **3e** in DMSO-d_6 (600 MHz).

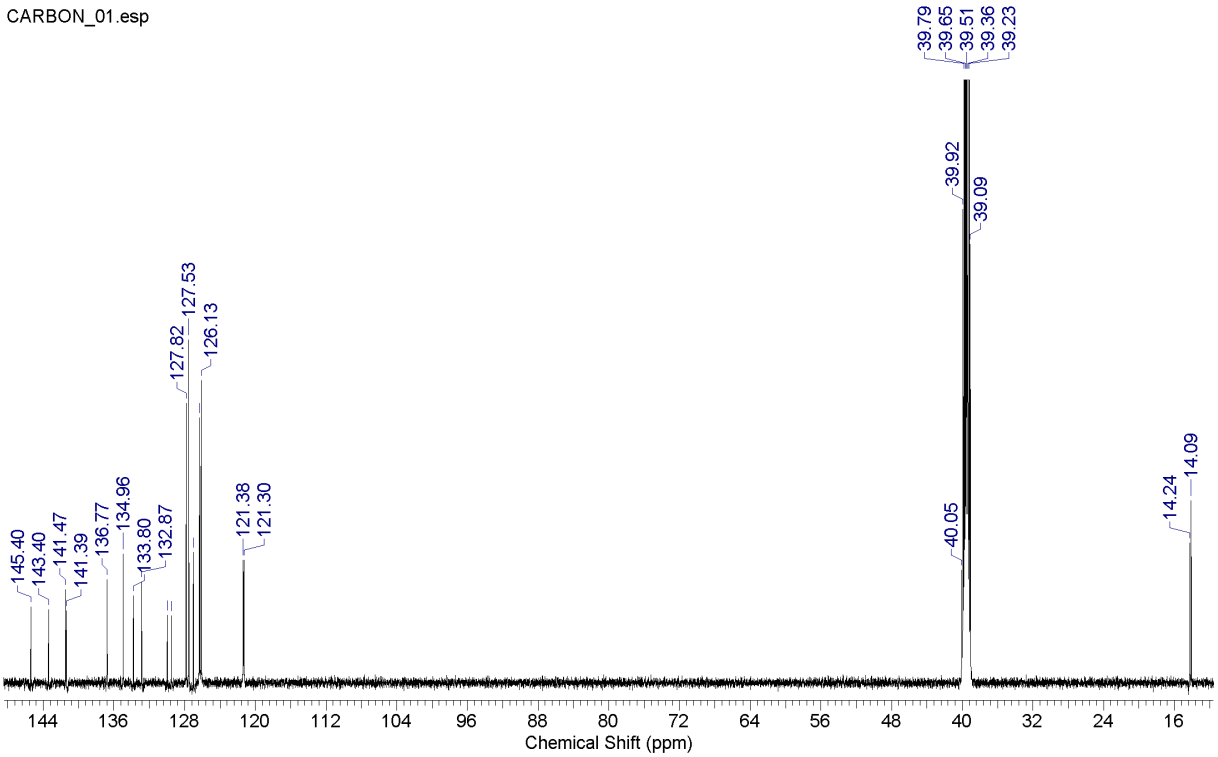

Figure S19. ^{13}C-NMR spectrum of compound **3e** in DMSO-d_6 (150 MHz).

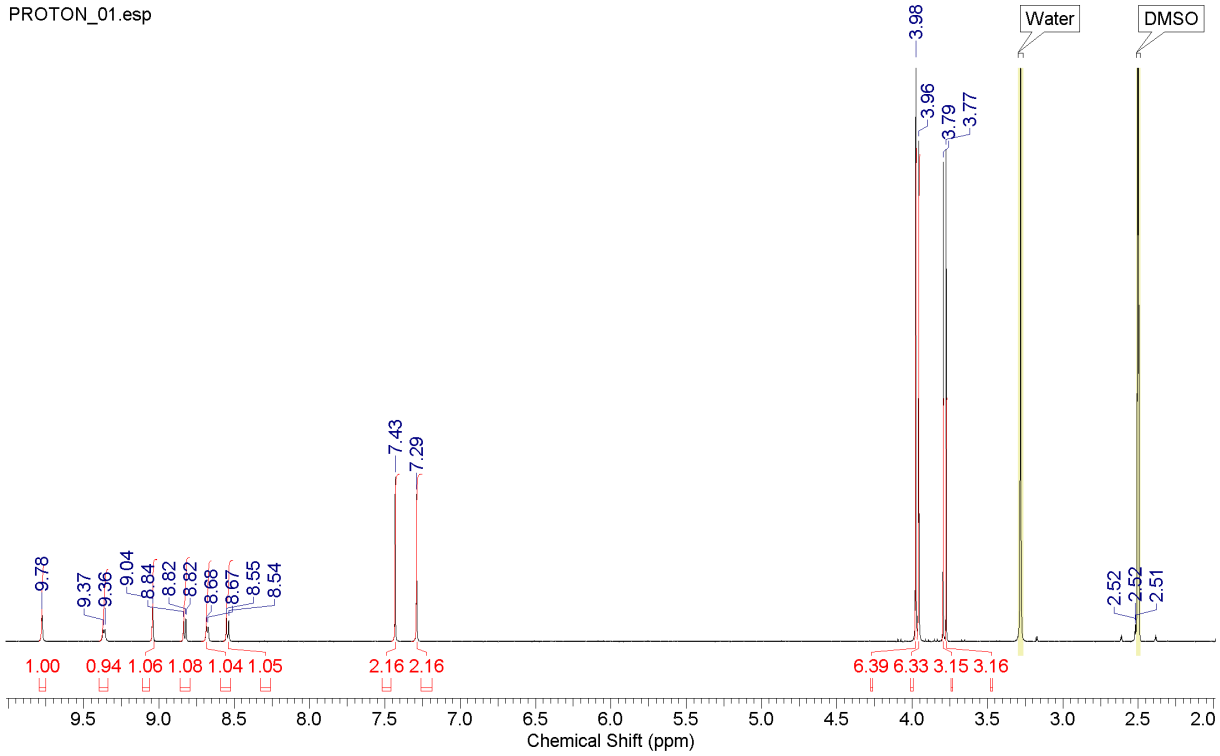

Figure S20. ^{1}H-NMR spectrum of compound **3f** in DMSO-d_6 (600 MHz).

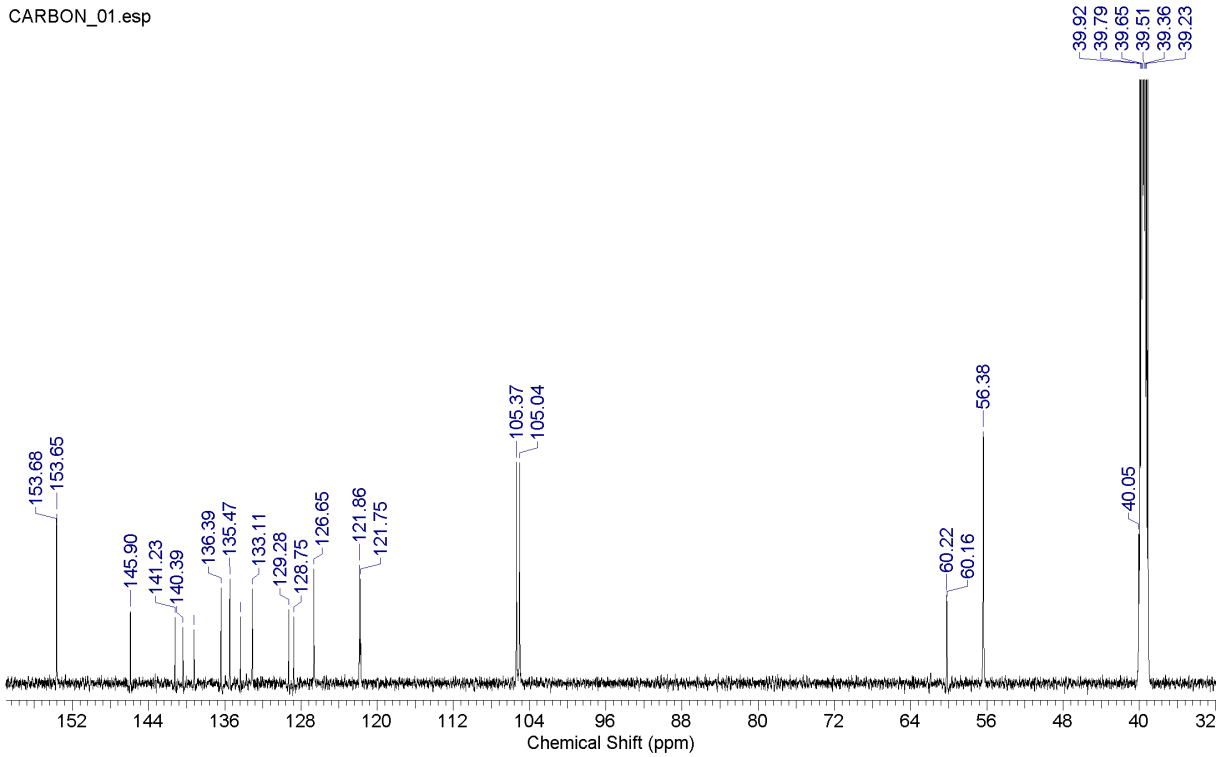

Figure S21. ^{13}C-NMR spectrum of compound **3f** in DMSO-d_6 (150 MHz).

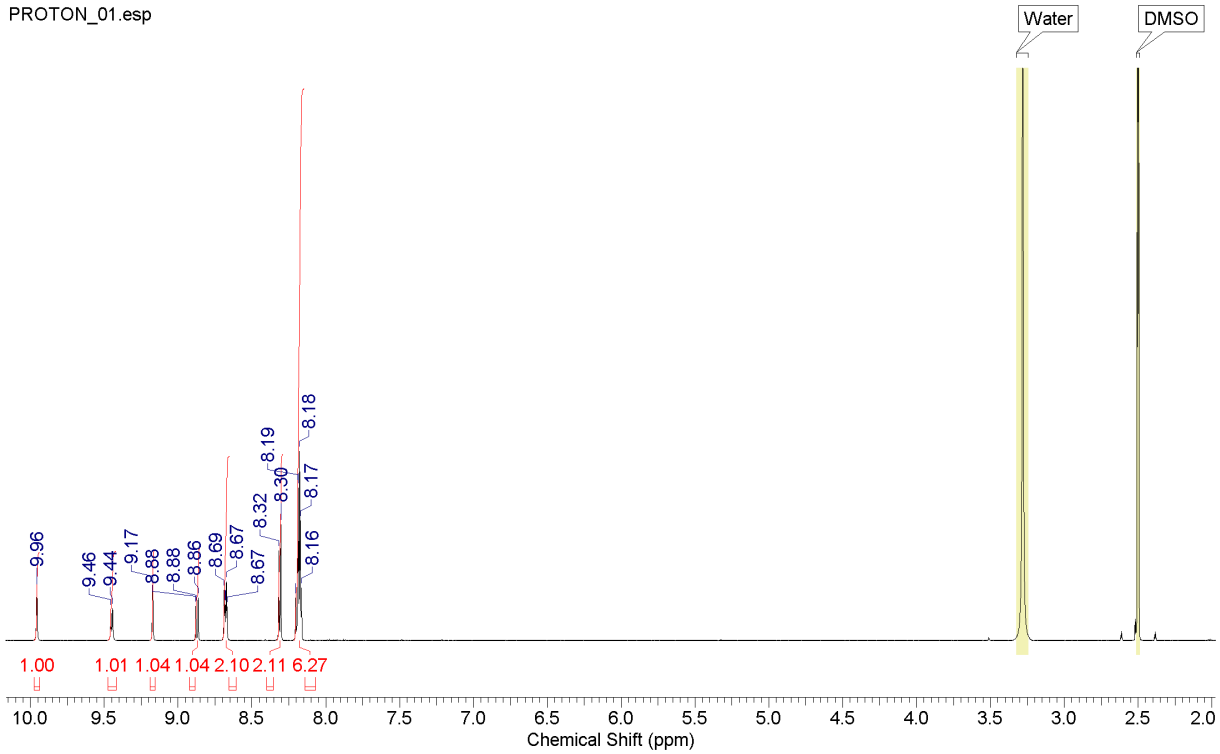

Figure S22. ^{1}H-NMR spectrum of compound **3g** in DMSO-d_6 (600 MHz).

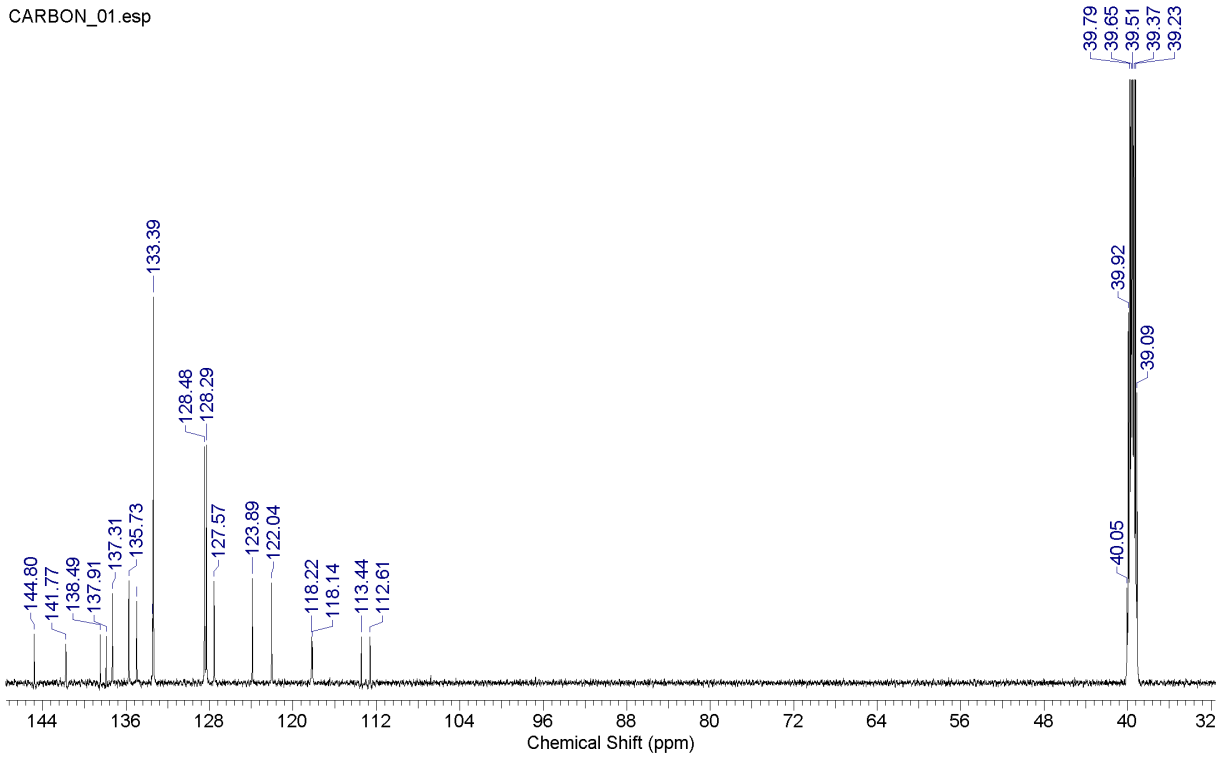

Figure S23. ^{13}C-NMR spectrum of compound **3g** in DMSO-d_6 (150 MHz).

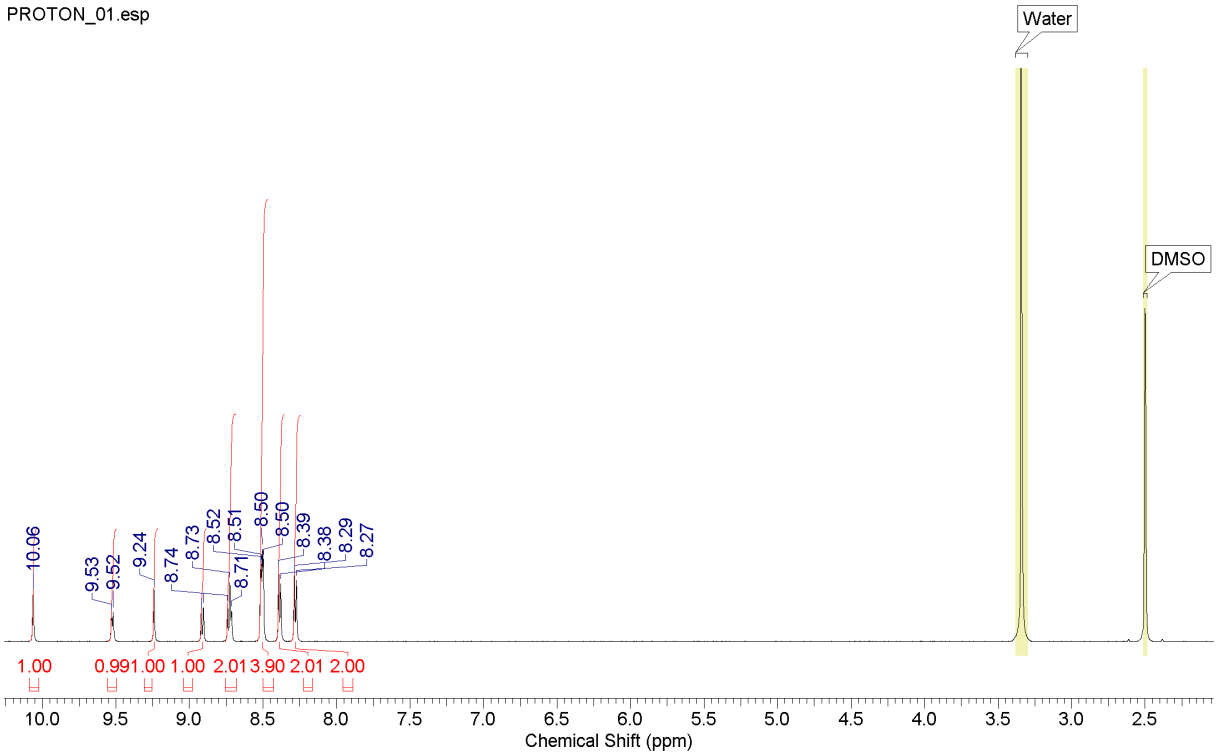

Figure S24. ^{1}H-NMR spectrum of compound **3h** in DMSO-d_6 (600 MHz).

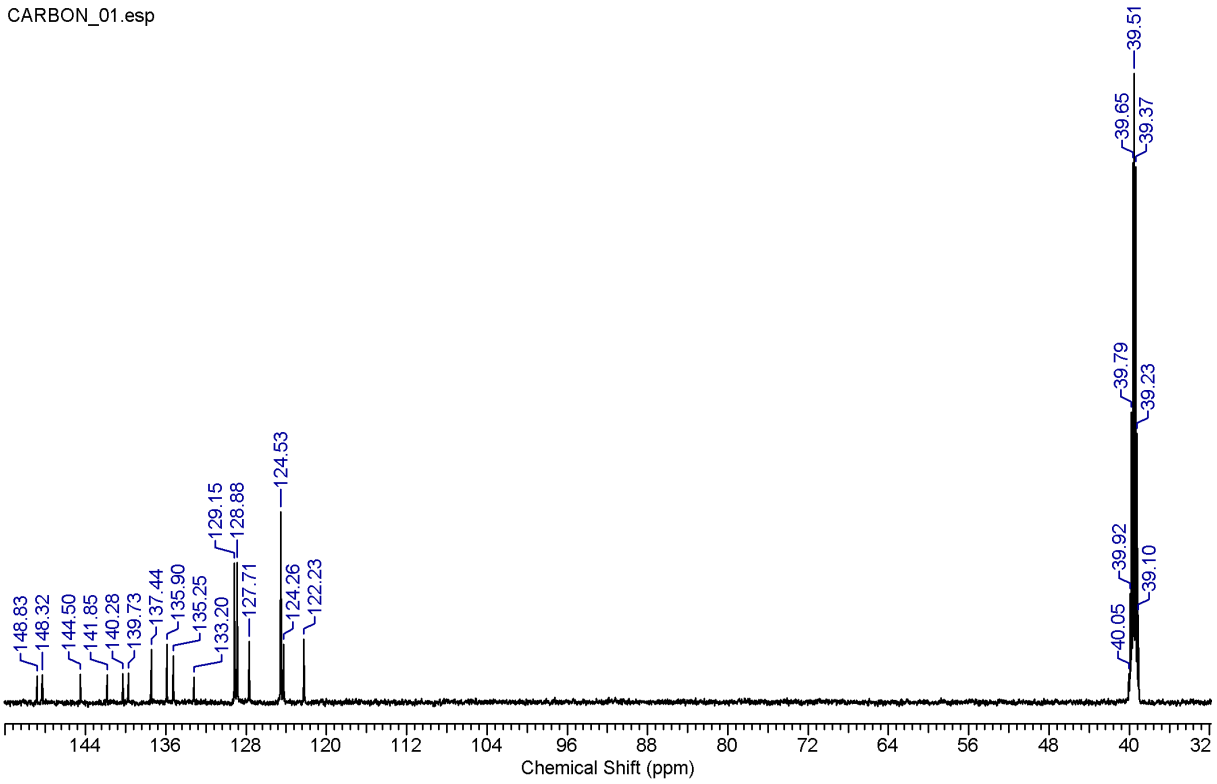

Figure S25. ^{13}C-NMR spectrum of compound **3h** in DMSO-d_6 (150 MHz).

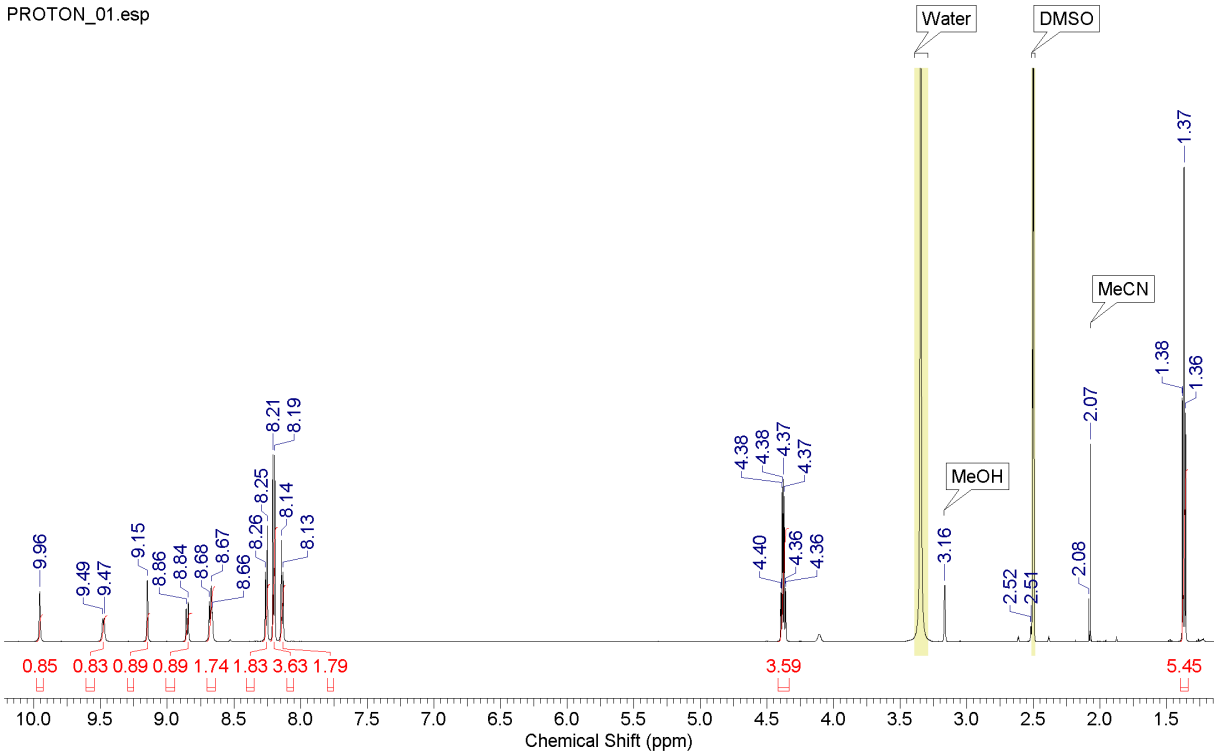

Figure S26. ^{1}H-NMR spectrum of compound **3i** in DMSO-d_6 (600 MHz).

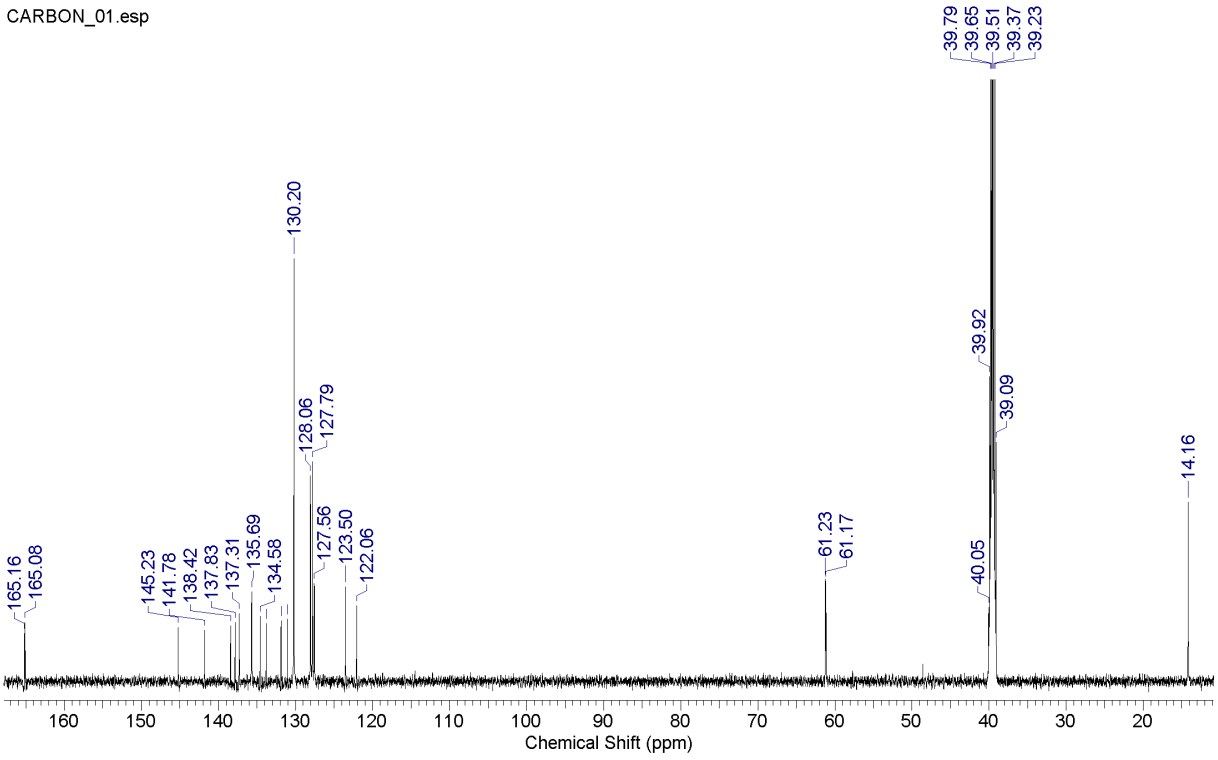

Figure S27. ^{13}C-NMR spectrum of compound **3i** in DMSO-d_6 (150 MHz).

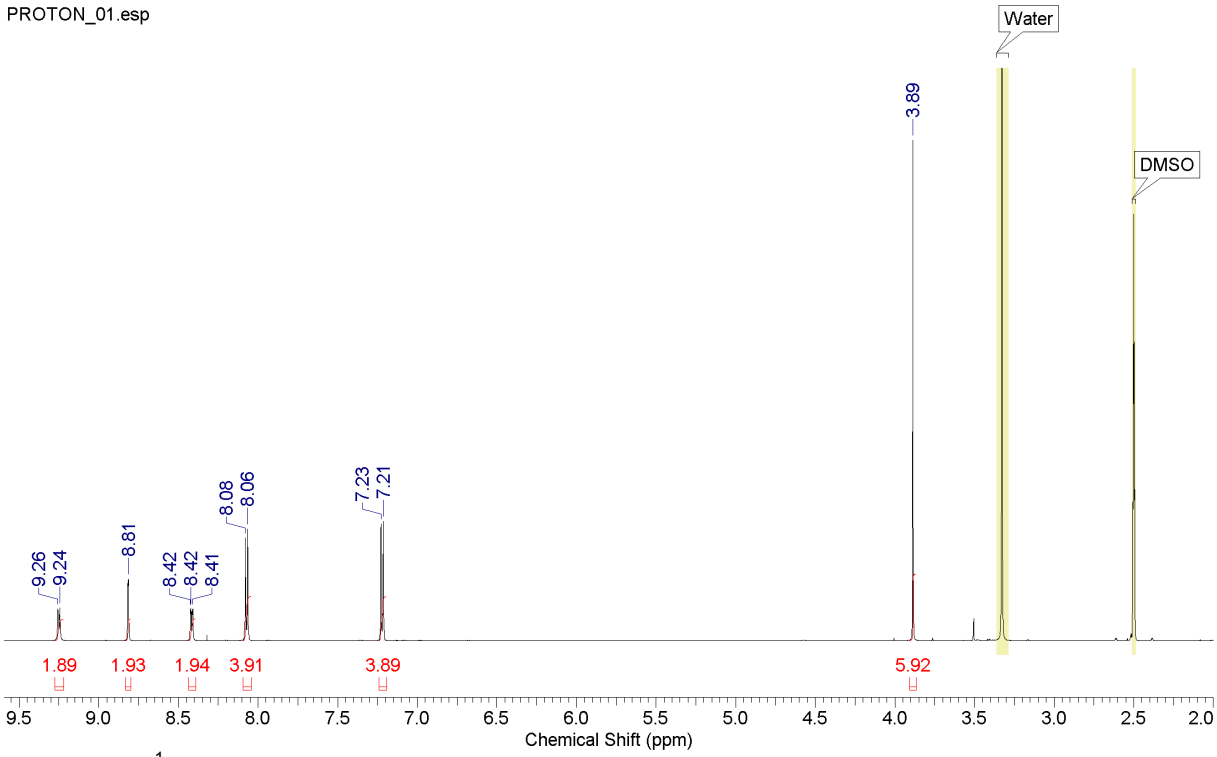

Figure S28. ^{1}H-NMR spectrum of compound **3j** in DMSO-d_6 (600 MHz).

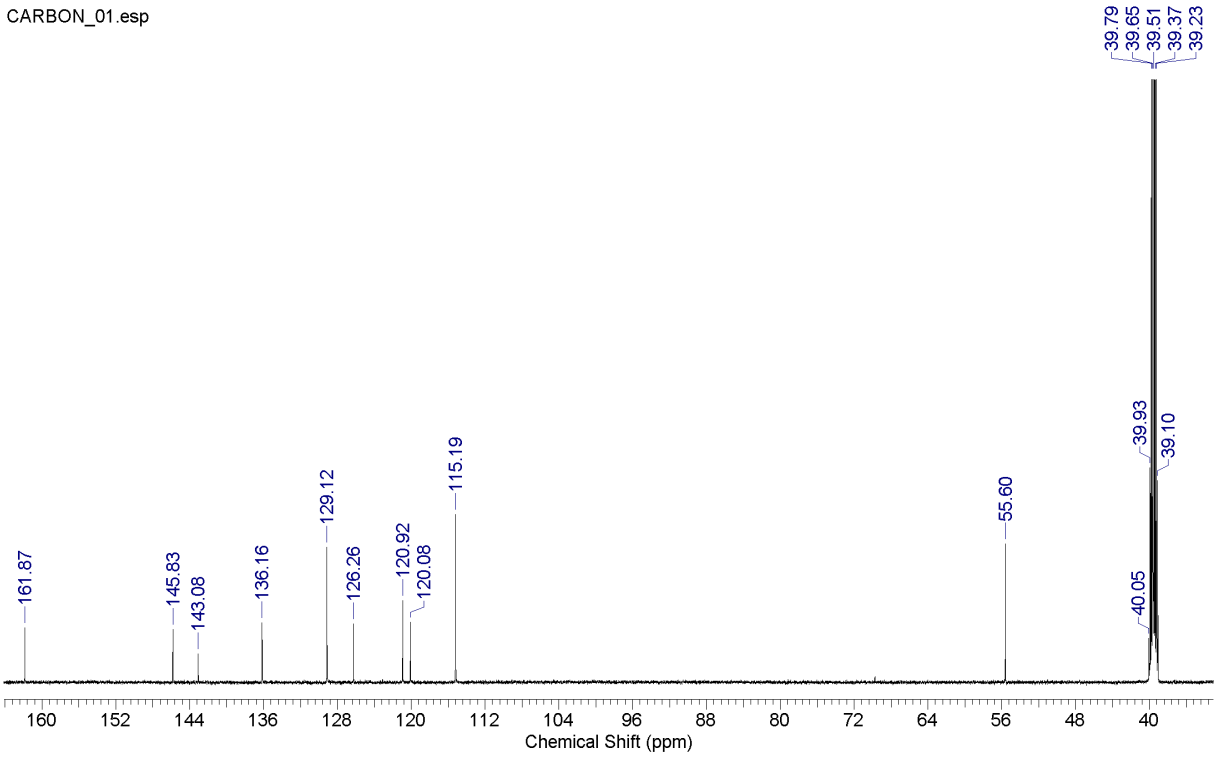

Figure S29. ^{13}C-NMR spectrum of compound **3j** in DMSO-d_6 (150 MHz).